

## STATISTICAL PROPERTIES OF MAGNETIC FIELDS IN INTRANETWORK

E.V. Khomenko<sup>(1)</sup>, M. Collados<sup>(2)</sup>, A. Lagg<sup>(3)</sup>, S.K. Solanki<sup>(3)</sup>, and J. Trujillo Bueno<sup>(2)</sup><sup>(1)</sup> *Main Astronomical Observatory NAS, 03680 Kyiv, Zabolotnogo str. 27, Ukraine, E-mail: khomenko@mao.kiev.ua*<sup>(2)</sup> *Instituto de Astrofísica de Canarias, E-38200, La Laguna, Tenerife, Spain, E-mail: mcv@ll.iac.es / jtb@ll.iac.es*<sup>(3)</sup> *Max-Planck-Institut für Aeronomie, 37191 Katlenburg-Lindau, Germany, E-mail: solanki@linmpi.mpg.de / lagg@linmpi.mpg.de*

## ABSTRACT

We report a study of the quiet sun's magnetic field based on high-resolution infrared spectropolarimetric observations (TIP/VTT). We find that in almost 50% of the pixels Stokes  $V$  and in 15% the Stokes  $Q$  and/or  $U$  profiles have a signal above  $10^{-3}$ . The statistical properties of the mainly intranetwork field sampled by these observations are presented, showing that most of the observed fields are weak (the field strength distribution peaks at 350 G and has a FWHM of 300 G) with very few kG features. The magnetized regions occupy a very small fill fractions (about 2%). The field changes properties on a granular spatial scales and the size of the patches formed by similar profiles is close to  $1''$ . Most of the parameters of the observed polarization profiles show correlations with granulation parameters.

## 1. INTRODUCTION

What is the nature of the magnetic field in the intranetwork? Do the measured weak fluxes comprise spatially unresolved tiny intense fluxtubes or they are intrinsically weak? Are they randomly directed and moved by the turbulent granular flows?

Observations of the field in the intranetwork are scarce and the results are contradictory. The first spectral observations in circular polarization in the intranetwork were performed by Keller et al. [5] who showed evidence that these fields are below kG. Lin [7], followed by Lin and Rimmele [8] directly measured Zeeman splitting in the intranetwork with the help of circular polarized spectra of  $1.56 \mu\text{m}$  IR lines. They reveal sub-kilogauss field strength and a new weak "granular" component of the magnetic field in the quiet region that was probably of turbulent origin. Other hypothesis like MISMA scenario by Sánchez Almeida and Lites [13] lead to strong mixed-polarity fields occupying small fill fractions. However, Lites [9] argues in his most recent paper from the analysis of the same data as Sánchez Almeida and Lites [13], that the two components are present

in the intranetwork - one is similar to the "granular" fields of Lin and Rimmele [8] and another is a diffuse extremely weak larger-scale component which the Hanle effect is sensitive to.

This paper presents preliminary results from the analysis of high resolution, low noise spectropolarimetric observations of the full Stokes vector of Fe I  $\lambda 15648 \text{ \AA}$  and Fe I  $\lambda 15653 \text{ \AA}$  lines taken with the Tenerife Infrared Polarimeter (TIP) attached to the German VTT in Tenerife. We use these IR lines for the measurement of the magnetic field strength directly from the splitting of the Stokes  $V$   $\sigma$ -components without involving line formation.

## 2. OBSERVATIONS

Full Stokes spectropolarimetric images were taken using the Tenerife Infrared Polarimeter (TIP, [10]) attached to the echelle spectrograph of the 70 cm German VTT operating at the Spanish Observatorio del Teide (Tenerife) in two independent observing runs. The first dataset was obtained on July 29<sup>th</sup>, 2000 and the second on September 5<sup>th</sup>, 2000. In both cases, a quiet region located at disk center was scanned, and the presence of plage or network magnetic signals were intentionally avoided to increase the statistics of the observed weak intranetwork fields, located inside supergranules.

The observed spectral range covered the two Fe I lines  $15648 \text{ \AA}$  ( $g = 3$ ) and  $15653 \text{ \AA}$  ( $g = 1.6$ ), with a sampling of  $29.1 \text{ m\AA/px}$ . The slit covered  $38''$  on the sun, with a sampling of  $0.4''$ . In both campaigns, the sun was scanned perpendicularly to the slit at steps of  $0.4''$ . The field of view thus measured had a size of  $20'' \times 38''$  in July, and about  $40'' \times 38''$  in September. This last region, due to its larger size, included a small patch of network.

The seeing conditions were rather good and stable during the first observing campaign, and slightly worse during the second campaign. The instantaneous granulation contrast was between 5 and 6% in the first case and approximately 3% in the second case. A correlation tracker [1] was used to stabilize

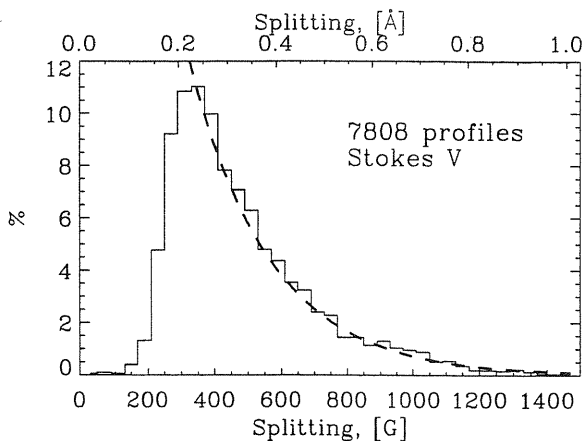


Figure 1. Histogram of Stokes  $V$   $\sigma$ -component splittings. Only 2-lobe profiles were used. Upper horizontal axis indicates splitting in  $\text{\AA}$ . Dashed line: the fit by an exponent  $A \exp(-B/B_0)$  to the right part of the histogram.

the image and to make the scan. To increase the signal to noise ratio, 120 sets of four images were on-line added up in July, and 100 in September (corresponding to total integration times of 50 and 60 seconds, at each position of the slit). After this integration, the noise in the Stokes  $Q$ ,  $U$ , and  $V$  spectral images was about  $2-3 \times 10^{-4}$  in units of the continuum intensity. The data reduction procedure included the removal of crosstalk between the Stokes parameters [2]. No crosstalk between Stokes  $Q$ ,  $U$  and  $V$  larger than of a few percent remains in the data. The position of zero velocity wavelength was defined as an average of the intensity minimum positions taken at the pixels where the magnetic signal was undetected, i.e. below noise.

In almost 50% of the pixels Stokes  $V$  and in 15% the Stokes  $Q$  and/or  $U$  profiles have a signal above the threshold level of  $10^{-3}$  (in the units of  $I_c$ ). The amount of linear polarization indicates that the observed fields have a broad range of inclinations. The Stokes  $V$  and  $Q/U$  profiles were classified using a single value decomposition approach [see for details our forthcoming paper 6]. This classification shows that 57% of the observed pixels with signal contain fields with the dominant single value. In 10% of the magnetic features several components with the same polarity, but different field strengths and velocities are present. Areas with mixed polarities and different velocities occupy about 30% in total. The spatial distribution of the magnetic signal shows that profiles of different classes (having different velocities, splitting, asymmetries) are clustered together and form patches. The statistical distribution of the profiles of different classes is similar in July and September, except for the fact that in September more homogeneous and less mixed polarity fields were observed. In general, the spatial scale of the field changes is

close to the granular scale, it is of about  $0.95''$  in the July data and  $1.25''$  in the September data.

### 3. MAGNETIC FIELD PROPERTIES

For the determination of Zeeman splitting, amplitudes, velocities, and other line parameters discussed below we used only profiles of regular shape with a well-defined zero-crossing and two lobes (for Stokes  $V$ ) or 3 lobes (Stokes  $Q$  and  $U$ ). We applied a data analysis procedure similar to that of Lin [7]. Each observed  $V$  profile was represented by a sum of two Gaussians. We have fitted both spectral lines and have 8 free parameters of the fit. The minimum detectable field strength with our fitting procedure is about 200 G which is limited by the width of the spectral lines (equivalent width  $140 \text{ m}\text{\AA}$  for the  $g = 3$  line). The uncertainty of the field strength determination increases for smaller splitting (see the discussion by Lin [7]) and the results should be considered an estimate.

#### 3.1. Magnetic field strength

Fig. 1 shows a histogram of the splitting of the Stokes  $V$  profiles in our data. The histogram peaks at 350 G. The intranetwork fields in our observations show very few kG features. The field strength values are in agreement with [5, 7, 8]. The tail of the distribution goes up to the field strengths about 1200 G, likely due to some remainings of a network piece in the September data. The number of profiles cuts rapidly near 200 G and its maximum is reached close to this value, so that the absence of lower fields in the histogram may be a consequence of the limitations of the analysis procedure. The preliminary results from the inversion of the July dataset using SIR inversion code [12] give a shape of the distribution of the field strengths that is similar to one obtained from the Gaussian fit algorithm [see 3], but the values of the field strength are lower. The number of pixels with a given magnetic field strength increases as this decreases. The shape of the histogram is nearly exponential (see the fit by an exponent shown in Fig. 1). A significant fraction of the field is below 350 G. This value is close to the equipartition field strength value of 200-400 G for the case the turbulent pressure of the convective motions supports the magnetic field concentrations.

We found hints that the splitting is larger in the dark intergranular lanes. The right panel of Fig. 2 demonstrates this result. Here the continuum intensity contrast (Stokes  $I$ ) was measured at points with appreciable signal in Stokes  $V$ . Only the July dataset was used because of the better seeing. The data from September show a similar but weaker tendency. Despite the large standard deviation, the binned data show a clear tendency: the field increases from about 450 G to 600 G as the continuum intensity of the feature decreases from 1.02 to 0.96. Another indication of the concentration of the field in intergranular lanes is that there are more data points with significant  $V$

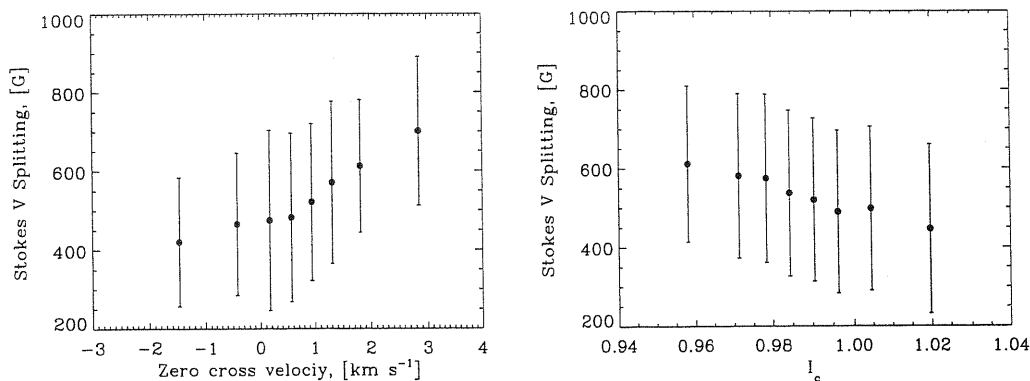


Figure 2. The Stokes  $V$  splitting as a function of zero crossing velocity (left panel) and continuum Stokes  $I$  intensity (right panel). 7808 2-lobed Stokes  $V$  profiles were used. Values of the splitting are binned into 9 intervals with an equal number of points. Error bars show the standard deviation within each interval.

signal at the darker pixels ( $I_c < 1$ ). Since we considered only pixels with the amplitude of the signal in Stokes  $V$  above the threshold, it means there is a less intense magnetic field in the bright granular pixels. At the same time, the Stokes  $V$  splitting increases with the increase of the zero-crossing velocity. The field is larger where the downflow is stronger (left panel of Fig. 2) The intensification of the magnetic field takes place when the flow of material is downward and the reverse process is observed when the flow is upward.

### 3.2. Filling factor and flux

The amplitudes of the polarization signal are very weak. The Stokes  $V$  amplitudes vary from below 0.001 up to 0.01 (in the units of  $I_c$ ). This speaks for a low filling factor of the observed field. Since the magnetic field strengths are also small, the influence of the magnetic field on the thermodynamical properties of the plasma should not be large. We assume that the thermodynamical properties of the atmosphere inside and outside magnetized regions are the same. Then, we can estimate the filling factor from the following relation:

$$f = \frac{2V}{(I_c - I_0) \cos \gamma}, \quad (1)$$

where  $V$  is the amplitude of the  $V$  profile  $\sigma$ -component taken from the Gaussian fit,  $I_c$  is the continuum intensity,  $I_0$  is the minimum residual intensity and  $\gamma$  is the inclination angle, estimated using the relation:

$$\frac{V}{\sqrt{Q^2 + U^2}} = \frac{\cos \gamma}{\sin^2 \gamma}, \quad (2)$$

where  $Q$ ,  $U$  and  $V$  are the amplitudes obtained from the Gaussian fit. This expression is only valid for a weak line (the two observed spectral lines are near this limit). The values of the filling factor obtained

vary up to 8%, but most of them are lower than 2%. Such values can be an underestimate, because the values of the Stokes  $V$  amplitudes returned by the Gaussian fit become less reliable with decreasing of splitting (and, thus field strength). It is difficult to separate the effect of the increase of the amplitude due to increase of the field strength and the filling factor in the weak field regime. We believe the actual values of the filling factor to be larger, but the field strength to be smaller, leading however to similar flux values. This conclusion is supported by the results of the SIR inversion of the same dataset [see 3]. We estimate the flux by

$$\phi = fR^2B \cos \gamma, \quad (3)$$

where  $R$  is the radius of our resolution element ( $0.38'' \times 0.38''$ ),  $B$  is the magnetic field strength. The scatter plot of the flux vs. splitting is given in Fig. 3. This figure is similar to the results found by Lin [7]. It demonstrates that the scattering of fluxes increases with the fields strength. Also, the field strength increases with the amount of flux, in agreement with Solanki et al. [15]

Assuming the average value of the filling factor to be  $f = 0.02$ , we obtain the size of the magnetic elements to be about 40 km. This value is only half that found by [8].

## 4. DISCUSSION AND CONCLUSIONS

High resolution spectropolarimetric observations show that the field in the intranetwork is highly dynamic. Concentrations of field appear in intergranular lanes and are accompanied by strong downflows. However, kG concentrations are not formed. The fluxes are extremely low, the lowest observed so far with the help of Zeeman effect. These weak fields occupy only about 2% of the area.

Conclusions on the nature of these fields are not easy to draw. Their properties are close to the "granular" magnetic fields seen by Lin and Rimmele [8]

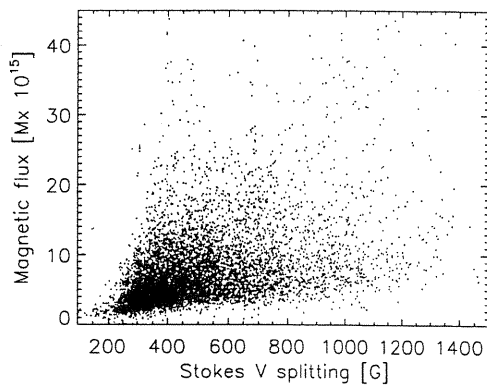


Figure 3. Scatter plot of the magnetic flux and splitting.

and Lites [9]. Our observations are at the limit of the sensitivity which can be reached with the Zeeman effect. They do not exclude the presumption that even more weak fields are present in between the observed flux concentrations, which cannot be detected with the present techniques.

Realistic magnetoconvection simulations are starting to be available at present [see 14]. They show that the convective collapse mechanism is responsible for the formation of the magnetic field concentrations. The initially homogeneous field is swept to the intergranular lanes where the flows converge and further intensification is reached by a thermal instability. Our observations are in agreement with the picture of the magnetic flux expulsion [11] into down-flow regions. But, the estimated width of the concentrations formed, that is 40 km, is smaller than the photon mean free path, and such flux tubes should have thermodynamical properties not very different from the surrounding atmosphere. Further intensification of the field according to the convective collapse instability will not be effective for such small field dimensions. An alternative scenario for the appearance of the magnetic field in the quiet sun is the local dynamo mechanism in the simulations by Emonet and Cattaneo [4]. In these idealized simulations (no compressibility of the fluid, ionization and radiative transfer included) a random seed field is enhanced by dynamo action and turbulent motions concentrate the magnetic field into discrete structures that evolve with the granulation time scale. Emonet and Cattaneo [4] show that this mechanism is able to generate kG fields. The finite spatial resolution in observations will result in the appearance of these fields in the form of small patches of different polarity. Emonet and Cattaneo [4] demonstrated that with decreasing spatial resolution most information on the strong fields will be lost and the filling factor that can be obtained from observations for such fields becomes smaller. Thus, the information of the random component of the magnetic field will be lost in observations.

Our results (the weakness of the field, exponential shape of the histogram of the field strength distribution, dependence on granulation parameters, variations of inclination) point toward a turbulent character of the intranetwork field. However, the mechanisms of its generations are unclear.

## ACKNOWLEDGMENTS

E. Khomenko is grateful to the organizers of the "SOLMAG" conference for the IAU travel grant. Discussions and help by R. Kostik is kindly acknowledged.

## REFERENCES

1. Ballesteros, E., Collados, M., Bonet, J. A., Lorenzo, F., Viera, T., Reyes, M., and Rodríguez Hidalgo, I.: 1996, *Astron. Astrophys. Suppl. Ser.* **115**, 353
2. Collados, M.: 1999, in B. Schmieder, A. Hofmann, and J. Staude (Eds.), *Solar magnetic fields and oscillations*, Vol. 184, ASP Conf. Series, 3
3. Collados, M.: 2001, in M. Sigwarth (Ed.), *Advanced solar polarimetry: Theory, observation and instrumentation*, Vol. 236, ASP Conf. Series, 255
4. Emonet, T. and Cattaneo, F.: 2001, in M. Sigwarth (Ed.), *Advanced solar polarimetry: Theory, observation and instrumentation*, Vol. 236, ASP Conf. Series, 355
5. Keller, C. U., Deubner, F.-L., Egger, U., Fleck, B., and Povel, H. P.: 1994, *Astron. Astrophys.* **286**, 626
6. Khomenko, E. V., Collados, M., Solanki, S. K., Lagg, A., and Trujillo Bueno, J.: 2002, *Astron. Astrophys.* in preparation
7. Lin, H.: 1995, *Astrophys. J.* **446**, 421
8. Lin, H. and Rimmele, T.: 1999, *Astrophys. J.* **514**, 448
9. Lites, B. W.: 2002, *Astrophys. J.* in press
10. Martínez Pillet, V. and *et al.*: 1999, in T. R. Rimmele, K. S. Balasubramaniam, and R. R. Radick (Eds.), *High resolution solar physics: theory, observations and techniques*, Vol. 183, ASP Conf. Series, 264
11. Parker, E. N.: 1963, *Astrophys. J.* **138**, 552
12. Ruiz Cobo, B. and del Toro Iñiesta, J. C.: 1992, *Astrophys. J.* **398**, 375
13. Sánchez Almeida, J. and Lites, B. W.: 2000, *Astrophys. J.* **532**, 1215
14. Schüssler, M.: 2001, in M. Sigwarth (Ed.), *Advanced solar polarimetry: Theory, observation and instrumentation*, Vol. 236, ASP Conf. Series, 343
15. Solanki, S. K., Zufferey, D., Lin, H., Rüedi, I., and Kuhn, J. R.: 1996, *Astron. Astrophys.* **310**, L33